

KIAS-P00021  
 OCHA-PP-156  
 hep-ph/0005118  
 December 2, 2024

# Probing the MSSM Higgs Boson Sector with Explicit CP Violation through Third Generation Fermion Pair Production at Muon Colliders

Eri Asakawa<sup>1</sup>, S.Y. Choi<sup>2</sup> and Jae Sik Lee<sup>3</sup>

<sup>1</sup>*Graduate School of Humanities and Sciences, Ochanomizu University,  
 1-1 Otsuka 2-chome, Bunkyo, Tokyo 112-8610, Japan*

<sup>2</sup>*Department of Physics, Chonbuk National University, Chonju 561-756, Korea*

<sup>3</sup>*Korea Institute for Advanced Study, Seoul 130-012, Korea*

## Abstract

We perform a systematic study of the production of a third-generation fermion-pair,  $\mu^+\mu^- \rightarrow f\bar{f}$  for  $f = \tau^-, b$ , and  $t$  in the minimal supersymmetric standard model (MSSM) with explicit CP violation, which is induced radiatively by soft trilinear interactions related to squarks of the third generation. We classify all the observables for probing the CP property of the Higgs bosons constructed by the initial muon beam polarization along with the unpolarized final fermions and with the final-fermion polarization configuration of equal helicity, respectively. The observables allow for complete determination of CP property of the neutral Higgs bosons. The interference between the Higgs boson and gauge boson contributions also could provide a powerful method for the determination of the CP property of two heavy Higgs bosons in the top-quark pair production near the energy region of the Higgs-boson resonances. For the lightest Higgs-boson mass there is no sizable interference between scalar and vector contributions for the determination of the CP property of the lightest Higgs boson. We give a detailed numerical analysis to show how the radiatively-induced CP violation in the Higgs sector of the MSSM can be measured.

# 1 Introduction

Search for the Higgs bosons and the precise measurements on their properties, such as the masses, the decay widths and the decay branching ratios, are the most important subjects to study the mechanism of the electroweak symmetry breaking [1]. In the Standard Model (SM), only one physical neutral Higgs boson appears. On the other hand, models with multiple Higgs doublets have CP-even and odd neutral Higgs bosons as well as charged Higgs bosons, if CP is a good symmetry. Otherwise, the neutral Higgs bosons do not have to carry any definite CP-parity.

CP violation was observed in the neutral kaon system [2] and the violation in B-meson decays is strongly suggested by recent experiments [3]. In addition, CP violation constitutes one of the crucial ingredients for an efficient non-SM generation of the cosmological baryon asymmetry at the electroweak scale [4]. An appealing scheme of CP violation beyond the SM can be provided by models with an extended Higgs sector where the CP asymmetry is broken by the ground state of the Higgs potential. It has recently been realized that, even though the Higgs potential of the minimal supersymmetric SM (MSSM) is CP-invariant at the tree level, explicit CP violation in the mass matrices of the third generation squarks can induce sizable CP violation in the MSSM Higgs sector through loop corrections [5, 6, 7, 8, 9]. The CP violating phases for the third generation sfermions can be quite large, since they contribute to the electric dipole moments of the electron and neutron only at the two-loop level with no generation mixing in the sfermion sector [10]. As a result, although a one-loop effect, the induced CP violation in the MSSM Higgs sector can be large enough to significantly affect Higgs phenomenology at present and future colliders [5, 6, 11, 12, 13]. In this light, it is very important to examine the possibility of observing these Higgs bosons and investigating their properties in detail.

A muon collider is one of the ideal machines to look for the Higgs bosons and their properties, where  $\mu^+\mu^-$  pairs can be directly converted into neutral Higgs-boson resonances [14, 15]. Polarized muons can be used to detect the Higgs bosons and measure their properties such as masses, total widths, decay branching fractions and CP parities [16, 17]. In this paper, we present a general formalism and a detailed analysis for the Higgs-boson effects on the polarized cross section of the production process  $\mu^+\mu^- \rightarrow f\bar{f}$  ( $f = \tau^-, b$  and  $t$ ) using the initial muon beam polarization along with the unpolarized final fermions and with the final-fermion polarization configuration of equal helicity, respectively. It has been recently pointed out that the amplitudes for two Higgs states, a scalar and a pseudoscalar, can interfere with each other sizably if the helicities of the initial and final particles are properly fixed and if the mass difference of these Higgs bosons is at most of the same order as their decay widths [18]. We extend the work comprehensively in order to consider Higgs bosons of no definite CP-parity in the MSSM with explicit CP violation induced from the

third generation squark sectors.

The remainder of this article is organized as follows. Section 2 is devoted to a brief review of the explicit CP violation in the MSSM Higgs sector based on the work [8]. In section 3 we present the helicity amplitudes of the production of a fermion pair in  $\mu^+\mu^-$  collisions and give a comprehensive classification of the observables according to the CP and  $CP\tilde{T}$  transformation properties that are constructed by the initial muon beam polarization along with the final fermions of no polarization and of equal helicity, respectively. In section 4 we make a detailed numerical analysis based on a given parameter set so as to get a concrete estimate of the usefulness of the observables. Section 5 is devoted to a brief summary of our findings and to a conclusion.

## 2 Explicit CP Violation in the MSSM Higgs Sector

The existence of the non-trivial CP-violating phases in the MSSM is due to the breakdown of supersymmetry so that the CP-violating phases appear in the soft-breaking parameters and the mixing among sparticles due to the electroweak gauge symmetry breaking. There are three well-known sources of CP violation in the MSSM [19]. The first is related to the two Higgs-boson doublets present in the model since both the  $\mu$  parameter in the superpotential and the soft breaking parameter  $m_{12}^2$  can be complex. Secondly, there are three more phases of the complex masses of the  $U(1)_Y$ ,  $SU(2)_L$  and  $SU(3)_C$  gauginos of the SM gauge group. Thirdly, the other CP-violating phases originate from the flavor sector of the MSSM Lagrangian, either in the scalar soft mass matrices or the trilinear matrices.

The CP-violating phases associated with the off-diagonal terms of the trilinear matrices are, however, strongly suppressed by the same mechanism required to suppress the flavor changing neutral current effects. Therefore, all these flavor-changing CP-violating phases are neglected in the present work such that the scalar soft mass matrices and trilinear parameters are flavor diagonal and the complex trilinear terms are proportional to the corresponding fermion Yukawa couplings. Clearly, the Yukawa interactions of the third-generation quarks and squarks play the most significant role in radiative corrections to the Higgs sector. In this section, we give a brief review of the calculation [8] of the Higgs-boson mass matrix based on the full one-loop effective potential, valid for all values of the relevant third-generation soft-breaking parameters.

The MSSM contains two Higgs doublets  $H_1$ ,  $H_2$ , with hypercharges  $Y(H_1) = -Y(H_2) = -1/2$ . Here we are only interested in the neutral components, which we write as

$$H_1^0 = \frac{1}{\sqrt{2}}(\phi_1 + ia_1); \quad H_2^0 = \frac{e^{i\xi}}{\sqrt{2}}(\phi_2 + ia_2), \quad (1)$$

where  $\phi_{1,2}$  and  $a_{1,2}$  are real fields. The constant phase  $\xi$  can be set to zero at tree level, but will in general become non-zero once loop corrections are included.

The mass matrix of the neutral Higgs bosons can be computed from the effective potential [20]

$$V_{\text{Higgs}} = \frac{1}{2}m_1^2(\phi_1^2 + a_1^2) + \frac{1}{2}m_2^2(\phi_2^2 + a_2^2) - |m_{12}^2|(\phi_1\phi_2 - a_1a_2)\cos(\xi + \theta_{12}) \\ - |m_{12}^2|(\phi_1a_2 + \phi_2a_1)\sin(\xi + \theta_{12}) + \frac{\hat{g}^2}{8}\mathcal{D}^2 + \frac{1}{64\pi^2}\text{Str}\left[\mathcal{M}^4\left(\log\frac{\mathcal{M}^2}{Q^2} - \frac{3}{2}\right)\right], \quad (2)$$

where we have allowed the soft breaking parameter  $m_{12}^2 = |m_{12}^2|e^{i\theta_{12}}$  to be complex, and we have introduced the quantities

$$\mathcal{D} = \phi_2^2 + a_2^2 - \phi_1^2 - a_1^2; \quad \hat{g}^2 = \frac{g^2 + g'^2}{4}, \quad (3)$$

where the symbols  $g$  and  $g'$  stand for the  $\text{SU}(2)_L$  and  $\text{U}(1)_Y$  gauge couplings, respectively.  $Q$  in Eq. (2) is the renormalization scale; the parameters of the tree-level potential, in particular the mass parameters  $m_1^2$ ,  $m_2^2$  and  $m_{12}^2$ , are running parameters, taken at scale  $Q$ . The potential (2) is then independent of  $Q$ , up to two-loop corrections.

The matrix  $\mathcal{M}$  is the field-dependent mass matrix of all modes that couple to the Higgs bosons. The by far dominant contributions come from the third generation quarks and squarks. The (real) masses of the former are given by

$$m_b^2 = \frac{1}{2}|h_b|^2(\phi_1^2 + a_1^2); \quad m_t^2 = \frac{1}{2}|h_t|^2(\phi_2^2 + a_2^2), \quad (4)$$

where  $h_b$  and  $h_t$  are the bottom and top Yukawa couplings. The corresponding squark mass matrices can be written as

$$\mathcal{M}_t^2 = \begin{pmatrix} m_Q^2 + m_t^2 - \frac{1}{8}\left(g^2 - \frac{g'^2}{3}\right)\mathcal{D} & -h_t^*[A_t^*(H_2^0)^* + \mu H_1^0] \\ -h_t[A_t H_2^0 + \mu^*(H_1^0)^*] & m_U^2 + m_t^2 - \frac{g'^2}{6}\mathcal{D} \end{pmatrix}; \\ \mathcal{M}_b^2 = \begin{pmatrix} m_Q^2 + m_b^2 + \frac{1}{8}\left(g^2 + \frac{g'^2}{3}\right)\mathcal{D} & -h_b^*[A_b^*(H_1^0)^* + \mu H_2^0] \\ -h_b[A_b H_1^0 + \mu^*(H_2^0)^*] & m_D^2 + m_b^2 + \frac{g'^2}{12}\mathcal{D} \end{pmatrix}. \quad (5)$$

Here,  $H_1^0$  and  $H_2^0$  are given by Eq. (1) while  $m_t^2$  and  $m_b^2$  are as in Eq. (4) and  $\mathcal{D}$  has been defined in Eq. (3). In Eq. (5)  $m_Q^2$ ,  $m_U^2$  and  $m_D^2$  are real soft breaking parameters,  $A_b$  and  $A_t$  are complex soft breaking parameters, and  $\mu$  is the complex supersymmetric Higgs(ino) mass parameter.

The calculation proceeds by plugging the field-dependent top/bottom-(s)quark mass eigenvalues into the potential (2). The mass matrix of the Higgs bosons (at vanishing external momentum) is then given by the matrix of second derivatives of this potential, computed at its minimum. In order to make sure that we are indeed in the minimum of the potential, we solve the stationarity relations, i.e. set the first derivatives of the potential to zero. This allows us to, e.g., express  $m_1^2$ ,  $m_2^2$  and  $m_{12}^2 \sin(\xi + \theta_{12})$  as functions of the vacuum expectation values (vevs) and the remaining parameters appearing in the loop-corrected Higgs potential. The equations  $\partial V_{\text{Higgs}}/\partial a_1 = 0$  and  $\partial V_{\text{Higgs}}/\partial a_2 = 0$  are linearly dependent, i.e. lead to only one constraint on parameters for  $\langle a_1 \rangle = \langle a_2 \rangle = 0$ ; the remaining vevs are defined through  $\langle \phi_1 \rangle^2 + \langle \phi_2 \rangle^2 = v^2 \simeq (246 \text{ GeV})^2$  and  $\langle \phi_2 \rangle / \langle \phi_1 \rangle = \tan \beta$ . The re-phasing invariant quantity  $|m_{12}^2| \sin(\xi + \theta_{12})$  is then determined by  $|m_{12}^2|$ ,  $m_{t_i}^2$  and  $m_{b_i}^2$  as well as by the re-phasing invariant quantities

$$\Delta_{\tilde{t}} = \frac{\Im(A_t \mu e^{i\xi})}{m_{t_2}^2 - m_{t_1}^2}; \quad \Delta_{\tilde{b}} = \frac{\Im(A_b \mu e^{i\xi})}{m_{b_2}^2 - m_{b_1}^2}, \quad (6)$$

which describe the amount of CP violation in the squark mass matrices.

The mass matrix of the neutral Higgs bosons can now be computed from the matrix of second derivatives of the potential (2), where (after taking the derivatives)  $m_1^2$ ,  $m_2^2$  and  $m_{12}^2 \sin(\xi + \theta_{12})$  are determined by the stationarity conditions. The massless state  $G^0 = a_1 \cos \beta - a_2 \sin \beta$  is the would-be Goldstone mode “eaten” by the longitudinal  $Z$  boson. We are thus left with a squared mass matrix  $\mathcal{M}_H^2$  for the three states  $a = a_1 \sin \beta + a_2 \cos \beta$ ,  $\phi_1$  and  $\phi_2$ . This matrix is real and symmetric, i.e. it has 6 independent entries. The diagonal entry for  $a$  reads:

$$\mathcal{M}_H^2|_{aa} = m_A^2 + \frac{3}{8\pi^2} \left\{ \frac{|h_t|^2 m_t^2}{\sin^2 \beta} g(m_{t_1}^2, m_{t_2}^2) \Delta_{\tilde{t}}^2 + \frac{|h_b|^2 m_b^2}{\cos^2 \beta} g(m_{b_1}^2, m_{b_2}^2) \Delta_{\tilde{b}}^2 \right\}, \quad (7)$$

and the CP-violating entries of the mass matrix, which mix  $a$  with  $\phi_1$  and  $\phi_2$  read:

$$\begin{aligned} \mathcal{M}_H^2|_{a\phi_1} = & \frac{3}{16\pi^2} \left\{ \frac{m_t^2 \Delta_{\tilde{t}}}{\sin \beta} \left[ g(m_{t_1}^2, m_{t_2}^2) (X_t \cot \beta - 2|h_t|^2 R_t) - \hat{g}^2 \cot \beta \log \frac{m_{t_2}^2}{m_{t_1}^2} \right] \right. \\ & \left. + \frac{m_b^2 \Delta_{\tilde{b}}}{\cos \beta} \left[ -g(m_{b_1}^2, m_{b_2}^2) (X_b + 2|h_b|^2 R'_b) + (\hat{g}^2 - 2|h_b|^2) \log \frac{m_{b_2}^2}{m_{b_1}^2} \right] \right\}, \end{aligned} \quad (8)$$

$$\begin{aligned} \mathcal{M}_H^2|_{a\phi_2} = & \frac{3}{16\pi^2} \left\{ \frac{m_t^2 \Delta_{\tilde{t}}}{\sin \beta} \left[ -g(m_{t_1}^2, m_{t_2}^2) (X_t + 2|h_t|^2 R'_t) + (\hat{g}^2 - 2|h_t|^2) \log \frac{m_{t_2}^2}{m_{t_1}^2} \right] \right. \\ & \left. + \frac{m_b^2 \Delta_{\tilde{b}}}{\cos \beta} \left[ g(m_{b_1}^2, m_{b_2}^2) (X_b \tan \beta - 2|h_b|^2 R_b) - \hat{g}^2 \tan \beta \log \frac{m_{b_2}^2}{m_{b_1}^2} \right] \right\}. \end{aligned} \quad (9)$$

where  $\Delta_{\tilde{t}}$  and  $\Delta_{\tilde{b}}$  are as in Eq. (6) and the function  $g(m_1^2, m_2^2)$  is given by

$$g(m_1^2, m_2^2) = 2 - \frac{m_1^2 + m_2^2}{m_1^2 - m_2^2} \log \frac{m_1^2}{m_2^2}. \quad (10)$$

The definition of the mass squared  $m_A^2$  and the dimensionless quantities  $X_{t,b}$ ,  $R_{t,b}$  and  $R'_{t,b}$  as well as the other CP-preserving entries of the mass matrix squared  $\mathcal{M}_H^2$  can be found in Ref. [8]. As noted earlier, the size of these CP-violating entries is controlled by  $\Delta_{\tilde{t}}$  and  $\Delta_{\tilde{b}}$ .

The real, symmetric matrix  $\mathcal{M}_H^2$  can be diagonalized with an orthogonal rotation  $O$ ;

$$O^T \mathcal{M}_H^2 O = \text{diag}(m_{H_1}^2, m_{H_2}^2, m_{H_3}^2), \quad (11)$$

with the ordering of  $m_{H_1} \leq m_{H_2} \leq m_{H_3}$  taken as a convention in the present work. Note that the loop-corrected neutral Higgs-boson sector is determined by fixing the values of various parameters;  $m_A$ ,  $\mu$ ,  $A_t$ ,  $A_b$ , a renormalization scale  $Q$ ,  $\tan \beta$ , and the soft-breaking third generation sfermion masses,  $m_{\tilde{Q}}$ ,  $m_{\tilde{U}}$ , and  $m_{\tilde{D}}$ . The radiatively induced phase  $\xi$  is no more an independent parameter and it can be absorbed into the definition of the  $\mu$  parameter so that the physically meaningful CP phases in the Higgs sector are the phases of the re-phasing invariant combinations  $A_t \mu e^{i\xi}$  and  $A_b \mu e^{i\xi}$ . This neutral Higgs-boson mixing changes the couplings of the Higgs fields to fermions, gauge bosons, and Higgs fields themselves so that the effects of CP violation in the Higgs sector can be probed through various processes [11, 12, 13].

### 3 Third Generation Fermion Production

#### 3.1 Production amplitudes

The couplings of the  $\gamma$  and the neutral gauge boson  $Z$  to fermions in the MSSM is described by the same interaction Lagrangian as in the SM:

$$\mathcal{L}_{V\mu\mu} = -e Q_f \bar{f} \gamma_\mu f A^\mu - \frac{e}{s_W c_W} \bar{f} [(T_{f3} - Q_f s_W^2) P_- - Q_f s_W^2 P_+] \gamma_\mu f Z^\mu, \quad (12)$$

with the chirality projection operators  $P_\pm = (1 \pm \gamma_5)/2$ , and those of the neutral Higgs-boson fields with leptons and quarks are described by the interaction Lagrangians

$$\begin{aligned} \mathcal{L}_{Hff} = & -\frac{h_l}{\sqrt{2}} \sum_{k=1}^3 \bar{\ell} [O_{2k} - i s_\beta O_{1k} \gamma_5] \ell H_k - \frac{h_d}{\sqrt{2}} \sum_{k=1}^3 \bar{d} [O_{2k} - i s_\beta O_{1k} \gamma_5] d H_k \\ & -\frac{h_u}{\sqrt{2}} \sum_{k=1}^3 \bar{u} [O_{3k} - i c_\beta O_{1k} \gamma_5] u H_k, \end{aligned} \quad (13)$$

where  $h_l$ ,  $h_d$ , and  $h_u$  are the lepton and quark Yukawa couplings:

$$h_l = \frac{g m_l}{\sqrt{2} m_W c_\beta}; \quad h_d = \frac{g m_d}{\sqrt{2} m_W c_\beta}; \quad h_u = \frac{g m_u}{\sqrt{2} m_W s_\beta}, \quad (14)$$

respectively. It is then clear that all the neutral Higgs bosons couple dominantly to the third generation fermions  $t$ ,  $b$  and  $\tau$  and they couple to a muon about 200 times more strongly than to an electron – the *primary reason* for having a muon collider.

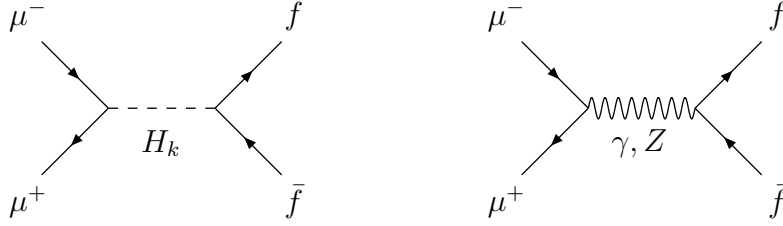


**Figure 1:** The mechanisms contributing to the process  $\mu^+\mu^- \rightarrow f\bar{f}$ ; three spin-0 neutral-Higgs-boson exchanges and spin-1  $\gamma$  and  $Z$  exchanges. Here, the index  $k$  is 1, 2 or 3.

The fermion pair production process  $\mu^+\mu^- \rightarrow f\bar{f}$  is generated by five  $s$ -channel mechanisms: spin-1  $\gamma$  and  $Z$  exchanges and three spin-0 neutral-Higgs-boson exchanges, cf. Fig. 1. The transition matrix element of the process

$$\mathcal{M} = \frac{S_{ab}}{s} [\bar{v}(\mu^+) P_a u(\mu^-)] [\bar{u}(f) P_b v(\bar{f})] + \frac{V_{ab}}{s} [\bar{v}(\mu^+) \gamma_\mu P_a u(\mu^-)] [\bar{u}(f) \gamma^\mu P_b v(\bar{f})], \quad (15)$$

can be expressed in terms of the scalar and vector bilinear charges,  $S_{ab}$  and  $V_{ab}$ , classified according to the chiralities  $a, b = \pm$  for the right-/left-handed chiralities of the associated muon and produced fermion currents, respectively. Here, the scalar bilinear charges are given by:

$$S_{ab} = -\frac{h_\mu h_f}{2} \sum_{k=1}^3 D_{H_k}(s) [O_{2k} - i a s_\beta O_{1k}] [S_k^f - i b \xi_\beta O_{1k}] - \frac{e^2 m_\mu m_f}{4 m_W^2 s_W^2} D_Z(s) T_{f3} ab, \quad (16)$$

where  $h_\mu$  and  $h_f$  are the initial muon and final fermion Yukawa couplings, respectively, and

$$D_{H_k}(s) = \frac{s}{s - m_{H_k}^2 + i m_{H_k} \Gamma_{H_k}}, \quad D_Z(s) = \frac{s}{s - m_Z^2 + i m_Z \Gamma_Z},$$

$$S_k^f = \begin{cases} O_{2k} \\ O_{3k} \end{cases}, \quad \xi_\beta = \begin{cases} s_\beta & \text{for } f = l \text{ or } d \\ c_\beta & \text{for } f = u \end{cases}. \quad (17)$$

On the other hand, the vector bilinear charges  $V_{ab}$  have the contributions only from the  $\gamma$  and  $Z$  boson exchanges:

$$V_{ab} = e^2 \left[ -Q_f + g_a^\mu g_b^f D_Z(s) \right], \quad (18)$$

where  $Q_f$  is the electric charge of the fermion,  $g_\pm^f$  denote the right/left-handed couplings of the  $Z$  boson to the fermions, respectively:

$$g_+^f = -Q_f \tan \theta_W, \quad g_-^f = -Q_f \tan \theta_W + \frac{T_{3f}}{s_W c_W}. \quad (19)$$

The vector bilinear charges  $V_{ab}$  are real in the approximation of neglecting the  $Z$  boson width  $\Gamma_Z$ , which is valid for the c.m. energy away from the  $Z$  boson pole.

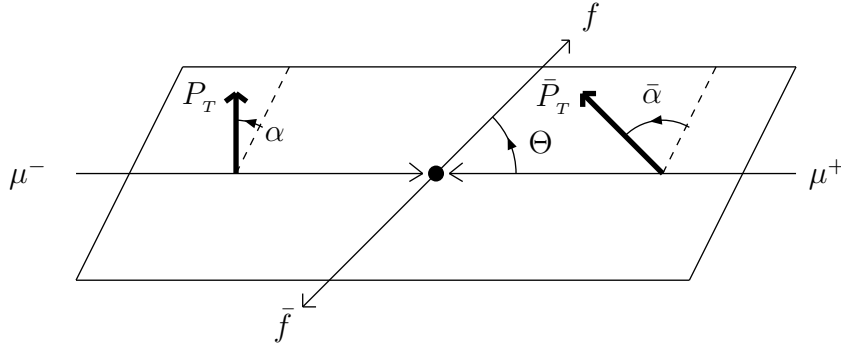


**Figure 2:** The schematic description of the production plane with the scattering angles  $\Theta$  and  $\Phi$  as well as the transverse polarization vectors  $P_T$  and  $\bar{P}_T$  with the azimuthal angles  $\alpha$  and  $\bar{\alpha}$  with respect to the scattering angle, respectively.

Defining the polar angle of the flight direction of the fermion  $f$  with respect to the  $\mu^-$  beam direction by  $\Theta$  (See Fig. 2), the explicit form of the production amplitude (15) can be evaluated in the helicity basis by the 2-component spinor technique of Ref. [21]. Denoting the  $\mu^- (\mu^+)$  helicity by the first (second) index, the  $f$  and  $\bar{f}$  helicities by the remaining two indices, then the general form of the helicity amplitude  $\langle \sigma \bar{\sigma}; \lambda \bar{\lambda} \rangle$ , consisting of a scalar helicity amplitude and a vector helicity amplitude, reads

$$\langle \sigma \bar{\sigma}; \lambda \bar{\lambda} \rangle = \langle \sigma \bar{\sigma}; \lambda \bar{\lambda} \rangle_s + \langle \sigma \bar{\sigma}; \lambda \bar{\lambda} \rangle_v, \quad (20)$$

where the scalar helicity amplitude  $\langle \sigma \bar{\sigma}; \lambda \bar{\lambda} \rangle_s$  is given by

$$\langle \sigma \bar{\sigma}; \lambda \bar{\lambda} \rangle_s = -\frac{1}{4} \sum_{ab} S_{ab} (a + \sigma \beta_\mu) (b - \lambda \beta) \delta_{\sigma \bar{\sigma}} \delta_{\lambda \bar{\lambda}}, \quad (21)$$



and the vector helicity amplitude  $\langle \sigma \bar{\sigma}; \lambda \bar{\lambda} \rangle_V$  by

$$\begin{aligned} \langle \sigma \bar{\sigma}; \lambda \bar{\lambda} \rangle_V = & -\frac{1}{4} \sum_{ab} V_{ab} \left\{ (1 + a\sigma\beta_\mu)(1 + b\lambda\beta)(\lambda\sigma + \cos\Theta) \delta_{\sigma,-\bar{\sigma}} \delta_{\lambda,-\bar{\lambda}} \right. \\ & - \frac{4m_\mu m_f}{s} (ab - \sigma\lambda \cos\Theta) \delta_{\sigma\bar{\sigma}} \delta_{\lambda\bar{\lambda}} \\ & - \frac{2m_\mu}{\sqrt{s}} (1 + b\lambda\beta)(\sigma \sin\Theta) \delta_{\sigma\bar{\sigma}} \delta_{\lambda,-\bar{\lambda}} \\ & \left. + \frac{2m_f}{\sqrt{s}} (1 + a\alpha\beta_\mu)(\lambda \sin\Theta) \delta_{\sigma,-\bar{\sigma}} \delta_{\lambda\bar{\lambda}} \right\}, \end{aligned} \quad (22)$$

respectively, with  $a, b = \pm$ ,  $\beta_\mu = \sqrt{1 - 4m_\mu^2/s}$  and  $\beta = \sqrt{1 - 4m_f^2/s}$ . However, the muon mass  $m_\mu$  ( $= 106$  MeV) is extremely small compared to the present experimental mass bound of approximately 100 GeV on the lightest Higgs boson so that one can safely neglect all the terms involving the kinematical muon mass\*. In the approximation, the scalar and vector helicity amplitudes can be written as:

**(i) Scalar helicity amplitudes:**

$$\begin{aligned} \langle ++; ++ \rangle_s &= \beta_+ S_{+-} - \beta_- S_{++}, \\ \langle ++; -- \rangle_s &= \beta_- S_{+-} - \beta_+ S_{++}, \\ \langle --; ++ \rangle_s &= \beta_- S_{-+} - \beta_+ S_{--}, \\ \langle --; -- \rangle_s &= \beta_+ S_{-+} - \beta_- S_{--}, \end{aligned} \quad (23)$$

where  $\beta_\pm = (1 \pm \beta)/2$ . At asymptotically high energies  $\beta_+ \rightarrow 1$  and  $\beta_- \rightarrow 0$ , and the other scalar helicity amplitudes vanish.

**(ii) Vector helicity amplitudes:**

$$\begin{aligned} \langle +-; ++ \rangle_V &= -\sqrt{\beta_+\beta_-} (V_{++} + V_{+-}) \sin\Theta, \\ \langle +-; +- \rangle_V &= -[\beta_+ V_{++} + \beta_- V_{+-}] (1 + \cos\Theta), \\ \langle +-; -+ \rangle_V &= +[\beta_- V_{++} + \beta_+ V_{+-}] (1 - \cos\Theta), \\ \langle +-; -- \rangle_V &= +\sqrt{\beta_+\beta_-} (V_{++} + V_{+-}) \sin\Theta, \\ \langle -+; ++ \rangle_V &= -\sqrt{\beta_+\beta_-} (V_{-+} + V_{--}) \sin\Theta, \\ \langle -+; +- \rangle_V &= +[\beta_+ V_{-+} + \beta_- V_{--}] (1 - \cos\Theta), \\ \langle -+; -+ \rangle_V &= -[\beta_- V_{-+} + \beta_+ V_{--}] (1 + \cos\Theta), \\ \langle -+; -- \rangle_V &= +\sqrt{\beta_+\beta_-} (V_{-+} + V_{--}) \sin\Theta, \end{aligned} \quad (24)$$

---

\*For consistency, the chirality-flipped  $Z$ -boson contributions to the scalar bilinear charges  $S_{ab}$ , which are also proportional to the muon mass kinematically, should be neglected in the massless muon limit.

and again the other vector helicity amplitudes vanish.

The CP transformation leads to the relation among the transition helicity amplitudes:

$$\langle \sigma \bar{\sigma}; \lambda \bar{\lambda} \rangle \xleftrightarrow{\text{CP}} +(-1)^{(\sigma-\bar{\sigma})/2}(-1)^{(\lambda-\bar{\lambda})/2} \langle -\bar{\sigma}, -\sigma; -\bar{\lambda}, -\lambda \rangle, \quad (25)$$

or equivalently for the scalar and vector helicity amplitudes:

$$\begin{aligned} \langle \pm \pm; \lambda \bar{\lambda} \rangle_s &\xleftrightarrow{\text{CP}} +(-1)^{(\lambda-\bar{\lambda})/2} \langle \mp \mp; -\bar{\lambda}, -\lambda \rangle_s, \\ \langle \pm \mp; \lambda \bar{\lambda} \rangle_v &\xleftrightarrow{\text{CP}} -(-1)^{(\lambda-\bar{\lambda})/2} \langle \pm \mp; -\bar{\lambda}, -\lambda \rangle_v. \end{aligned} \quad (26)$$

Only the simultaneous presence of the scalar and pseudoscalar couplings can lead to CP violation as can be explicitly checked in Eqs. (21) and (22). One additional useful classification is provided by the so-called “naive” time reversal  $\tilde{T}$ ; under the  $\text{CP}\tilde{T}$  transformations the helicity amplitudes are transformed as follows:

$$\begin{aligned} \langle \pm \pm; \lambda \bar{\lambda} \rangle_s &\xleftrightarrow{\text{CP}\tilde{T}} +(-1)^{(\lambda-\bar{\lambda})/2} \langle \mp \mp; -\bar{\lambda}, -\lambda \rangle_s^*, \\ \langle \pm \mp; \lambda \bar{\lambda} \rangle_v &\xleftrightarrow{\text{CP}\tilde{T}} -(-1)^{(\lambda-\bar{\lambda})/2} \langle \pm \mp; -\bar{\lambda}, -\lambda \rangle_v^*. \end{aligned} \quad (27)$$

We note that it is crucial to have finite  $Z$  or Higgs-boson widths for  $\text{CP}\tilde{T}$  violation. In this light, it is very useful to take into account the CP and  $\text{CP}\tilde{T}$  properties of any physical observable simultaneously so as to investigate not only CP violation itself but also the overlapping of any pair of three neutral Higgs boson resonances effectively.

### 3.2 Polarized production cross section

The matrix element squared for general (longitudinal or transverse) beam polarization can be computed either using standard trace techniques (employing general spin projection operators), or from the helicity amplitudes by a suitable rotation [21] from the helicity basis to a general spin basis. In the former case, neglecting the muon mass in the spin projection operators we can obtain the following approximated form for the  $\mu^\mp$  projection operators

$$\begin{aligned} \frac{1}{2}(\not{p} + m)(1 + \gamma_5 \not{s}) &\longrightarrow \frac{1}{2}(1 + P_L \gamma_5) \not{p} + \frac{1}{2}\gamma_5 P_T (\cos \alpha \not{p}_1 + \sin \alpha \not{p}_2) \not{p}, \\ \frac{1}{2}(\not{p} - m)(1 + \gamma_5 \not{s}) &\longrightarrow \frac{1}{2}(1 - \bar{P}_L \gamma_5) \not{p} + \frac{1}{2}\gamma_5 \bar{P}_T (\cos \bar{\alpha} \not{p}_1 + \sin \bar{\alpha} \not{p}_2) \not{p}. \end{aligned} \quad (28)$$

Equivalently in the helicity basis the polarization weighted matrix element squared is given by

$$\overline{\sum} |\mathcal{M}|^2 = \sum_{\sigma \sigma' \bar{\sigma} \bar{\sigma}'} \mathcal{M}_{\sigma \bar{\sigma}} \mathcal{M}_{\sigma' \bar{\sigma}'}^* \rho_{\sigma \sigma'}^- \rho_{\bar{\sigma} \bar{\sigma}'}^+ = \text{Tr} [\mathcal{M} \rho^+ \mathcal{M}^\dagger \rho^{-T}], \quad (29)$$

where  $\mathcal{M}_{\sigma\bar{\sigma}}$  ( $\sigma, \bar{\sigma} = \pm$ ) denotes the helicity amplitude for any given production process  $\mu^-(\sigma)\mu^+(\bar{\sigma}) \rightarrow X$  and the  $2 \times 2$  matrices  $\rho^\mp$  are the polarization density matrices for the initial  $\mu^\mp$  beams:

$$\rho^- = \frac{1}{2} \begin{pmatrix} 1 + P_L & P_T e^{-i\alpha} \\ P_T e^{i\alpha} & 1 - P_L \end{pmatrix}, \quad \rho^+ = \frac{1}{2} \begin{pmatrix} 1 + \bar{P}_L & -\bar{P}_T e^{i\bar{\alpha}} \\ -\bar{P}_T e^{-i\bar{\alpha}} & 1 - \bar{P}_L \end{pmatrix}. \quad (30)$$

Here,  $P_L$  and  $\bar{P}_L$  are the longitudinal polarizations of the  $\mu^-$  and  $\mu^+$  beams, while  $P_T$  and  $\bar{P}_T$  are the degrees of transverse polarization with  $\alpha$  and  $\bar{\alpha}$  being the azimuthal angles between the transverse polarization vectors and the momentum vector of  $f$  as shown in Fig. 2.

Applying the projection operators (28) or/and evaluating the trace (29) leads to the polarized matrix element squared of the form

$$\begin{aligned} \Sigma &\equiv \sum_{\lambda\bar{\lambda}} \sum_{\sigma\sigma'\bar{\sigma}\bar{\sigma}'} \langle \sigma\bar{\sigma}; \lambda\bar{\lambda} \rangle \langle \sigma'\bar{\sigma}'; \lambda\bar{\lambda} \rangle^* \rho_{\sigma\sigma'}^- \rho_{\bar{\sigma}\bar{\sigma}'}^+ \\ &= (1 - P_L \bar{P}_L) C_1 + (P_L - \bar{P}_L) C_2 \\ &\quad + (1 + P_L \bar{P}_L) C_3 + (P_L + \bar{P}_L) C_4 \\ &\quad + (P_T \cos \alpha + \bar{P}_T \cos \bar{\alpha}) C_5 + (P_T \sin \alpha + \bar{P}_T \sin \bar{\alpha}) C_6 \\ &\quad + (P_T \cos \alpha - \bar{P}_T \cos \bar{\alpha}) C_7 + (P_T \sin \alpha - \bar{P}_T \sin \bar{\alpha}) C_8 \\ &\quad + (P_L \bar{P}_T \cos \bar{\alpha} + \bar{P}_L P_T \cos \alpha) C_9 + (P_L \bar{P}_T \sin \bar{\alpha} + \bar{P}_L P_T \sin \alpha) C_{10} \\ &\quad + (P_L \bar{P}_T \cos \bar{\alpha} - \bar{P}_L P_T \cos \alpha) C_{11} + (P_L \bar{P}_T \sin \bar{\alpha} - \bar{P}_L P_T \sin \alpha) C_{12} \\ &\quad + P_T \bar{P}_T [\cos(\alpha + \bar{\alpha}) C_{13} + \sin(\alpha + \bar{\alpha}) C_{14}] \\ &\quad + P_T \bar{P}_T [\cos(\alpha - \bar{\alpha}) C_{15} + \sin(\alpha - \bar{\alpha}) C_{16}], \end{aligned} \quad (31)$$

where the coefficients  $C_n$  ( $n = 1 - 16$ ) are defined in terms of the helicity amplitudes by

$$\begin{aligned} C_1 &= \frac{1}{4} \sum_{\lambda, \bar{\lambda}=\pm} [|\langle +-, \lambda\bar{\lambda} \rangle|^2 + |\langle -+, \lambda\bar{\lambda} \rangle|^2], \quad C_2 = \frac{1}{4} \sum_{\lambda, \bar{\lambda}=\pm} [|\langle +-, \lambda\bar{\lambda} \rangle|^2 - |\langle -+, \lambda\bar{\lambda} \rangle|^2], \\ C_3 &= \frac{1}{4} \sum_{\lambda, \bar{\lambda}=\pm} [|\langle ++, \lambda\bar{\lambda} \rangle|^2 + |\langle --, \lambda\bar{\lambda} \rangle|^2], \quad C_4 = \frac{1}{4} \sum_{\lambda, \bar{\lambda}=\pm} [|\langle ++, \lambda\bar{\lambda} \rangle|^2 - |\langle --, \lambda\bar{\lambda} \rangle|^2], \\ C_5 &= \frac{1}{4} \Re \sum_{\lambda, \bar{\lambda}=\pm} (\langle ++, \lambda\bar{\lambda} \rangle - \langle --, \lambda\bar{\lambda} \rangle) (\langle -+, \lambda\bar{\lambda} \rangle - \langle +-, \lambda\bar{\lambda} \rangle)^*, \\ C_6 &= \frac{1}{4} \Im \sum_{\lambda, \bar{\lambda}=\pm} (\langle ++, \lambda\bar{\lambda} \rangle - \langle --, \lambda\bar{\lambda} \rangle) (\langle -+, \lambda\bar{\lambda} \rangle + \langle +-, \lambda\bar{\lambda} \rangle)^*, \\ C_7 &= \frac{1}{4} \Re \sum_{\lambda, \bar{\lambda}=\pm} (\langle ++, \lambda\bar{\lambda} \rangle + \langle --, \lambda\bar{\lambda} \rangle) (\langle -+, \lambda\bar{\lambda} \rangle + \langle +-, \lambda\bar{\lambda} \rangle)^*, \end{aligned}$$

$$\begin{aligned}
C_8 &= \frac{1}{4} \Im \sum_{\lambda, \bar{\lambda}=\pm} (\langle ++; \lambda \bar{\lambda} \rangle + \langle --; \lambda \bar{\lambda} \rangle) (\langle -+; \lambda \bar{\lambda} \rangle - \langle +-; \lambda \bar{\lambda} \rangle)^*, \\
C_9 &= \frac{1}{4} \Re \sum_{\lambda, \bar{\lambda}=\pm} (\langle ++; \lambda \bar{\lambda} \rangle + \langle --; \lambda \bar{\lambda} \rangle) (\langle -+; \lambda \bar{\lambda} \rangle - \langle +-; \lambda \bar{\lambda} \rangle)^*, \\
C_{10} &= \frac{1}{4} \Im \sum_{\lambda, \bar{\lambda}=\pm} (\langle ++; \lambda \bar{\lambda} \rangle + \langle --; \lambda \bar{\lambda} \rangle) (\langle -+; \lambda \bar{\lambda} \rangle + \langle +-; \lambda \bar{\lambda} \rangle)^*, \\
C_{11} &= -\frac{1}{4} \Re \sum_{\lambda, \bar{\lambda}=\pm} (\langle ++; \lambda \bar{\lambda} \rangle - \langle --; \lambda \bar{\lambda} \rangle) (\langle -+; \lambda \bar{\lambda} \rangle + \langle +-; \lambda \bar{\lambda} \rangle)^*, \\
C_{12} &= \frac{1}{4} \Im \sum_{\lambda, \bar{\lambda}=\pm} (\langle ++; \lambda \bar{\lambda} \rangle - \langle --; \lambda \bar{\lambda} \rangle) (\langle -+; \lambda \bar{\lambda} \rangle - \langle +-; \lambda \bar{\lambda} \rangle)^*, \\
C_{13} &= -\frac{1}{2} \Re \sum_{\lambda, \bar{\lambda}=\pm} [\langle -+; \lambda \bar{\lambda} \rangle \langle +-; \lambda \bar{\lambda} \rangle^*], \quad C_{14} = \frac{1}{2} \Im \sum_{\lambda, \bar{\lambda}=\pm} [\langle -+; \lambda \bar{\lambda} \rangle \langle +-; \lambda \bar{\lambda} \rangle^*], \\
C_{15} &= -\frac{1}{2} \Re \sum_{\lambda, \bar{\lambda}=\pm} [\langle --; \lambda \bar{\lambda} \rangle \langle ++; \lambda \bar{\lambda} \rangle^*], \quad C_{16} = \frac{1}{2} \Im \sum_{\lambda, \bar{\lambda}=\pm} [\langle --; \lambda \bar{\lambda} \rangle \langle ++; \lambda \bar{\lambda} \rangle^*]. \quad (32)
\end{aligned}$$

The production cross section is then given in terms of the distribution  $\Sigma$  in Eq. (31) by

$$\frac{d\sigma}{d\cos\Theta d\Phi} = \frac{N_C \beta}{64 \pi^2 s} \Sigma, \quad (33)$$

where  $N_C$  is the color factor of the final fermion; 3 for the top or bottom quark and 1 for the tau lepton. The dependence of the distribution  $\Sigma$  on the azimuthal angle  $\Phi$  of the production plane is encoded in the angles  $\alpha$  and  $\bar{\alpha}$ . If the azimuthal angle  $\Phi$  is measured with respect to the direction of the  $\mu^-$  transverse polarization vector, the  $\Phi$  dependence can be exhibited explicitly by taking

$$\alpha = -\Phi, \quad \bar{\alpha} = \eta - \Phi, \quad (34)$$

where  $\eta$  is the *rotational invariant* difference  $\bar{\alpha} - \alpha$  of the azimuthal angles of the  $\mu^+$  and  $\mu^-$  transverse polarization vectors with respect to the production plane. Clearly, only the six observables  $\{C_1, C_2, C_3, C_4, C_{15}, C_{16}\}$  can be measured independently of the azimuthal angle, but the other ten observables, in particular, the observables involving the SV correlations, require the reconstruction of the production plane.

The CP transformation on the polarization vectors of the initial muon beams corresponds to the simultaneous exchanges:

$$P_L \leftrightarrow -\bar{P}_L, \quad P_T \leftrightarrow \bar{P}_T, \quad \alpha \leftrightarrow \bar{\alpha}. \quad (35)$$

The CP relation (35) of the polarization vectors leads to the classification that the first 3 terms and the distributions  $\{C_5, C_6, C_{11}, C_{12}, C_{13}, C_{14}, C_{15}\}$  in Eq. (31) are CP-even while the other six distributions  $\{C_4, C_7, C_8, C_9, C_{10}, C_{16}\}$  are CP-odd. Among the CP-odd observables, the three observables  $\{C_4, C_7, C_9\}$  are  $\text{CPT}\tilde{\text{T}}$ -odd and the other three observables  $\{C_8, C_{10}, C_{16}\}$  are  $\text{CPT}\tilde{\text{T}}$ -even. Here, it will be noteworthy to emphasize again that one crucial requirement for having a large  $\text{CPT}\tilde{\text{T}}$ -odd observable is the presence of so-called CP-preserving re-scattering phases which can be provided by the Higgs boson propagators with relatively large widths in the present work.

### 3.3 Initial spin correlations

Let us now express the coefficients  $C_i$  ( $i = 1$  to 16) in terms of the scalar and vector bilinear and quartic charges [22] as well as the newly-introduced notations:

$$\begin{aligned} R_1 &= \sum_{ab} S_{ab}, & R_2 &= \sum_{ab} ab S_{ab}, & R_3 &= \sum_{ab} a S_{ab}, & R_4 &= \sum_{ab} b S_{ab}, \\ W_1 &= \sum_{ab} V_{ab}, & W_2 &= \sum_{ab} ab V_{ab}, & W_3 &= \sum_{ab} a V_{ab}, & W_4 &= \sum_{ab} b V_{ab}, \end{aligned} \quad (36)$$

which are to be employed for the interference between the scalar and vector contributions. It is worthwhile to note that both  $R_3$  and  $R_4$  vanish in the CP-invariant theory. The sixteen polarization distributions can be then classified as follows:

#### (i) Scalar-scalar (SS) correlations:

$$\begin{aligned} C_3[++] &= \frac{1}{2} \left[ (1 + \beta^2) S_1 - (1 - \beta^2) S_2 \right], \\ C_4[--] &= \frac{1}{2} \left[ (1 + \beta^2) S'_1 - (1 - \beta^2) S'_2 \right], \\ C_{15}[++] &= \frac{1}{2} \left[ (1 + \beta^2) S_4 - (1 - \beta^2) S_5 \right], \\ C_{16}[-+] &= \frac{1}{2} \left[ (1 + \beta^2) S'_4 - (1 - \beta^2) S'_5 \right], \end{aligned} \quad (37)$$

where the first and second signatures in the square brackets are for the CP and  $\text{CPT}\tilde{\text{T}}$  parities of the corresponding observable, respectively, and the relevant scalar quartic charges are defined as

$$\begin{aligned} S_1 &= \frac{1}{4} \left[ |S_{++}|^2 + |S_{--}|^2 + |S_{+-}|^2 + |S_{-+}|^2 \right], \\ S'_1 &= \frac{1}{4} \left[ |S_{++}|^2 + |S_{+-}|^2 - |S_{-+}|^2 - |S_{--}|^2 \right], \end{aligned}$$

$$\begin{aligned}
S_2 &= \frac{1}{2} \Re [S_{++} S_{+-}^* + S_{--} S_{-+}^*] , & S'_2 &= \frac{1}{2} \Re [S_{++} S_{+-}^* - S_{--} S_{-+}^*] , \\
S_4 &= \frac{1}{2} \Re [S_{++} S_{-+}^* + S_{--} S_{+-}^*] , & S'_4 &= \frac{1}{2} \Im [S_{++} S_{-+}^* - S_{--} S_{+-}^*] , \\
S_5 &= \frac{1}{2} \Re [S_{++} S_{--}^* + S_{+-} S_{-+}^*] , & S'_5 &= \frac{1}{2} \Im [S_{++} S_{--}^* + S_{+-} S_{-+}^*] , 
\end{aligned} \tag{38}$$

**(ii) Vector–vector (VV) correlations:**

$$\begin{aligned}
C_1[++] &= (1 + \beta^2 \cos^2 \Theta) V_1 + (1 - \beta^2) V_2 + 2\beta V_3 \cos \Theta, \\
C_2[++] &= (1 + \beta^2 \cos^2 \Theta) V'_1 + (1 - \beta^2) V'_2 + 2\beta V'_3 \cos \Theta, \\
C_{13}[++] &= \beta^2 \sin^2 \Theta V_4, \\
C_{14}[+-] &= \beta^2 \sin^2 \Theta V'_4,
\end{aligned} \tag{39}$$

where the quartic charges  $V_3$  and  $V'_3$  are given by

$$\begin{aligned}
V_3 &= \frac{1}{4} [ |V_{++}|^2 + |V_{--}|^2 - |V_{+-}|^2 - |V_{-+}|^2 ] , \\
V'_3 &= \frac{1}{4} [ |V_{++}|^2 - |V_{+-}|^2 + |V_{-+}|^2 - |V_{--}|^2 ] ,
\end{aligned} \tag{40}$$

and the other vector quartic charges are defined in the same way as the scalar quartic charges with the notation  $S$  replaced by  $V$  everywhere. We note that the scalar as well as vector quartic charges defined as an imaginary part of the bilinear–charge correlations might be non-vanishing only when there are complex CP–violating couplings or/and CP–preserving phases like re-scattering phases or finite widths of the intermediate particles. So, if there are no CP–preserving phases, non-vanishing values of these quartic charges signal CP violation in the given process.

**(iii) Scalar–vector (SV) correlations:**

$$\begin{aligned}
C_5[++] &= +\frac{m_f}{4\sqrt{s}} \beta \sin \Theta \Re(W_3 R_1^*), & C_6[+-] &= +\frac{m_f}{4\sqrt{s}} \beta \sin \Theta \Im(W_1 R_1^*), \\
C_7[--] &= -\frac{m_f}{4\sqrt{s}} \beta \sin \Theta \Re(W_1 R_3^*), & C_8[-+] &= -\frac{m_f}{4\sqrt{s}} \beta \sin \Theta \Im(W_3 R_3^*), \\
C_9[--] &= +\frac{m_f}{4\sqrt{s}} \beta \sin \Theta \Re(W_3 R_3^*), & C_{10}[-+] &= +\frac{m_f}{4\sqrt{s}} \beta \sin \Theta \Im(W_1 R_3^*), \\
C_{11}[++] &= +\frac{m_f}{4\sqrt{s}} \beta \sin \Theta \Re(W_1 R_1^*), & C_{12}[+-] &= +\frac{m_f}{4\sqrt{s}} \beta \sin \Theta \Im(W_3 R_1^*).
\end{aligned} \tag{41}$$

All the SV correlations are proportional to the mass of the final–state fermion divided by the c.m. energy so that they are strongly suppressed at high energies. In this light, they are sizable only in the production of the top–quark pair because of the largest fermionic mass.

### 3.4 Final spin correlations for Higgs interference effects

Various types of experimental observables by use of the initial muon polarization have been considered in the previous section for determining the CP character of the neutral MSSM Higgs bosons. In addition, spin correlations of  $t\bar{t}$  or  $\tau^+\tau^-$  in the final state can also probe the CP nature of the Higgs boson, independently of or combined with initial beam polarization. If the production plane or directly the momentum directions of two final fermions are determined, the secondary decays of the primary final state fermions can allow a complete analysis of their spin or helicity directions. However, even if the production plane is not reconstructed, one can obtain the fermion-pair polarization combination by statistically studying decay products from the correlated and polarized  $f\bar{f}$ . It is then natural that the production distribution needs to be integrated over the azimuthal angle  $\Phi$ .

The  $s$ -channel Higgs boson (spin-0) exchange populates the equal  $\mu^-\mu^+$  helicity combinations, i.e.  $\sigma = \bar{\sigma}$ . This results in the correlations of  $f\bar{f}$  polarization with  $\lambda = \bar{\lambda}$  by angular momentum conservation, while the SM background channels yield dominantly the  $(+-)$  or  $(-+)$  polarization combination. In addition, the CP transformation interchanges the  $(++)$  and  $(--)$  helicity configurations. In the light of these two arguments combined with the one in the previous paragraph, it will be valuable to consider the  $\Phi$ -independent polarization observable<sup>†</sup>:

$$\begin{aligned} \Delta &\equiv \sum_{\lambda} \sum_{\sigma\sigma'\bar{\sigma}\bar{\sigma}'} \lambda \langle \sigma\bar{\sigma}; \lambda\lambda \rangle \langle \sigma'\bar{\sigma}'; \lambda\lambda \rangle^* \rho_{\sigma\sigma'}^- \rho_{\bar{\sigma}\bar{\sigma}'}^+ \\ &= (1 + P_L \bar{P}_L) D_1 + (P_L + \bar{P}_L) D_2 + P_T \bar{P}_T [\cos \eta D_3 + \sin \eta D_4], \end{aligned} \quad (42)$$

where the distributions  $D_i$  ( $i = 1$  to 4) are defined in terms of the helicity amplitudes as

$$\begin{aligned} D_1[--] &= \frac{1}{4} \sum_{\lambda} \lambda \left[ |\langle ++; \lambda\lambda \rangle|^2 + |\langle --; \lambda\lambda \rangle|^2 \right], \\ D_2[++] &= \frac{1}{4} \sum_{\lambda} \lambda \left[ |\langle ++; \lambda\lambda \rangle|^2 - |\langle --; \lambda\lambda \rangle|^2 \right], \\ D_3[--] &= -\frac{1}{2} \Re \sum_{\lambda} \lambda [\langle --; \lambda\lambda \rangle \langle ++; \lambda\lambda \rangle^*], \\ D_4[+-] &= -\frac{1}{2} \Im \sum_{\lambda} \lambda [\langle --; \lambda\lambda \rangle \langle ++; \lambda\lambda \rangle^*], \end{aligned} \quad (43)$$

where the first and second signatures in the square brackets are for the CP and  $\text{CPT}$  parities of the corresponding observable.

---

<sup>†</sup>In principle, there can exist the  $\gamma$  and  $Z$ -exchange terms corresponding to the polarization combinations  $(1 - P_L \bar{P}_L)$  and  $(P_L - \bar{P}_L)$  of the initial  $\mu^+\mu^-$  beams. However, those terms turn out to be zero for the real vector and axial-vector couplings in the approximation of neglecting the  $Z$ -boson width.

### 3.5 CPT-even and odd combinations of Higgs-boson propagators

The CPT parity of each observable plays a crucial role in determining the interference pattern of the Higgs bosons among themselves and with the  $\gamma$  and  $Z$  bosons appearing in the observable; every CPT-even (odd) observable involving only the scalar contributions depends on the real (imaginary) part of the combination  $D_{H_k} D_{H_l}^*$  of each pair of two Higgs-boson propagators. The CPT-odd observable  $C_{14}$  involving only the vector contributions is negligible because the  $Z$ -boson width effect is significantly small for the energy far from the  $Z$ -boson pole. When the  $Z$ -boson width is neglected, all the vector couplings are real. As a result, the interference terms between the scalar and vector contributions depends on the real or imaginary parts of the Higgs-boson propagators  $D_{H_k}$  itself.

For the sake of discussion in the following, let us introduce for the real and imaginary parts the abbreviated notations:

$$\begin{aligned}\mathcal{S}_{kl} &\equiv \Re[D_{H_k} D_{H_l}^*] = \frac{(s - m_{H_k}^2)(s - m_{H_l}^2) + m_{H_k} m_{H_l} \Gamma_{H_k} \Gamma_{H_l}}{[(s - m_{H_k}^2)^2 + m_{H_k}^2 \Gamma_{H_k}^2][(s - m_{H_l}^2)^2 + m_{H_l}^2 \Gamma_{H_l}^2]}, \\ \mathcal{D}_{kl} &\equiv \Im[D_{H_k} D_{H_l}^*] = \frac{(s - m_{H_k}^2) m_{H_l} \Gamma_{H_l} - (s - m_{H_l}^2) m_{H_k} \Gamma_{H_k}}{[(s - m_{H_k}^2)^2 + m_{H_k}^2 \Gamma_{H_k}^2][(s - m_{H_l}^2)^2 + m_{H_l}^2 \Gamma_{H_l}^2]}.\end{aligned}\quad (44)$$

It is worthwhile to note two points; (a) the denominator reveals a typical two-pole structure so that the Higgs-boson contributions are greatly enhanced at the poles; (b) the numerator of  $\mathcal{S}_{kl}$  is negative in the middle of two resonances with a mass splitting larger than their typical widths but positive otherwise, while the numerator of  $\mathcal{D}_{kl}$  is always positive (negative) if  $m_{H_l} \geq m_{H_k}$  ( $m_{H_k} \geq m_{H_l}$ ) and linearly increasing (decreasing) if  $m_{H_l} \Gamma_{H_l} \geq m_{H_k} \Gamma_{H_k}$  ( $m_{H_k} \Gamma_{H_k} \geq m_{H_l} \Gamma_{H_l}$ ), respectively.

On the other hand, the SV interference terms depend on the real and imaginary parts of each Higgs-boson propagators  $D_{H_k}$ , the form of which is given by

$$\Re[D_{H_k}] = \frac{s - m_{H_k}^2}{(s - m_{H_k}^2)^2 + m_{H_k}^2 \Gamma_{H_k}^2}, \quad \Im[D_{H_k}] = -\frac{m_{H_k} \Gamma_{H_k}}{(s - m_{H_k}^2)^2 + m_{H_k}^2 \Gamma_{H_k}^2}.\quad (45)$$

Note that the real part changes its sign whenever the c.m. energy crosses the pole, but the imaginary part is always negative.

Combining the coefficients from the mixing matrix elements with those propagator-dependent parts enables us to make a straightforward qualitative understanding of the  $\sqrt{s}$  dependence of each observable. This will be demonstrated in detail in the following section with a concrete numerical example.



## 4 Numerical Results

We are now ready to present some numerical results. It is known that loop-induced CP violation in the Higgs sector can only be large if both  $|\mu|$  and  $|A_t|$  (or  $|A_b|$ , if  $\tan\beta \gg 1$ ) are sizable [5, 6, 7, 8]. We therefore choose  $|A_t| = |A_b| = 2m_{\tilde{Q}}$ . For definiteness we will present results only for the  $t\bar{t}$  mode by taking  $\tan\beta = 3, 10$  when probing the region around two heavy Higgs-boson resonances, but we will give a qualitative description of probing the CP property of the lightest Higgs boson. We take the running Yukawa couplings by including the QCD loop effects depending on the gluino mass properly. Since for moderate values of  $\tan\beta$  the contributions from the (s)bottom sector are still quite small, our results are not sensitive to  $m_{\tilde{D}}$  and  $A_b$ ; we therefore fix  $m_{\tilde{D}} = m_{\tilde{U}} = m_{\tilde{Q}}$ , although different values for the SU(2) doublet and singlet soft breaking squark masses,  $m_{\tilde{Q}} \neq m_{\tilde{U}}$  are allowed, and also take equal phases for  $A_t$  and  $A_b$ . Since we are basically interested in distinguishing the CP non-invariant Higgs sector from the CP invariant one, we take for the re-phasing-invariant phase  $\Phi_{A\mu}$  of  $A_{t,b}\mu e^{i\xi}$  two values; 0 (CP invariant case) and  $\pi/2$  (maximally CP violating case). On the other hand, we fix for simplicity the other real mass parameters and couplings except for  $\tan\beta$  as follows:

$$\begin{aligned} m_A &= 0.4 \text{ TeV}, \quad |A_{t,b}| = 1.0 \text{ TeV}, \quad |\mu| = 1.0 \text{ TeV}, \\ m_{\tilde{g}} &= 0.5 \text{ TeV}, \quad m_{\tilde{Q}} = m_{\tilde{U}} = m_{\tilde{D}} = 0.5 \text{ TeV}. \end{aligned} \quad (46)$$

Finally, we take for the top and bottom quark running masses  $\bar{m}_t(m_t) = 165 \text{ GeV}$  and  $\bar{m}_b(m_b) = 4.2 \text{ GeV}$ . For the given  $m_A$  much larger than  $m_Z$ , two neutral Higgs bosons have almost degenerate masses:

$$\begin{aligned} \tan\beta = 3, \Phi_{A\mu} = 0 & : m_{H_2} = 400.0 \text{ GeV}, \quad m_{H_3} = 400.4 \text{ GeV}, \\ \tan\beta = 3, \Phi_{A\mu} = \frac{\pi}{2} & : m_{H_2} = 396.6 \text{ GeV}, \quad m_{H_3} = 404.5 \text{ GeV}, \\ \tan\beta = 10, \Phi_{A\mu} = 0 & : m_{H_2} = 397.5 \text{ GeV}, \quad m_{H_3} = 400.0 \text{ GeV}, \\ \tan\beta = 10, \Phi_{A\mu} = \frac{\pi}{2} & : m_{H_2} = 397.3 \text{ GeV}, \quad m_{H_3} = 400.5 \text{ GeV}. \end{aligned} \quad (47)$$

As a result, a significant overlapping, i.e. interference between two Higgs-boson resonances is expected.

In the previous section, we have listed 16 polarization observables constructed solely by initial muon polarizations under the assumption that the production plane is (at least statistically) reconstructed, and 4 additional polarization observables by combining initial muon polarizations and final equal helicity configurations only for the case when the production plane does not have to be explicitly reconstructed. For some polarization observables it is also important to experimentally identify the electric charges of the produced fermion pair from their decay products. Taking into account all these requirements naturally leads us to

the following classification; for the energy range around the heavy Higgs boson resonances the production of a top quark pair is recommended to be used (when the heavy Higgs–boson masses are larger than twice the top–quark mass), and for the energy close to the lightest Higgs mass, the tau lepton or bottom quark pairs are recommended to be considered<sup>‡</sup>

## 4.1 Two heavy Higgs bosons for top–pair production

In the MSSM two heavy Higgs bosons are (almost) degenerate with a mass splitting comparable to or less than their widths for  $M_A \gg m_Z$  as in the case of the parameter set (46), and one of them is CP–even and the other CP–odd in the CP invariant theory. However, the CP–violating neutral Higgs–boson mixing can cause a mass splitting larger than their typical widths and it can lead to several significant non–vanishing CP–odd observables, in particular, in the  $t\bar{t}$  mode. In this section, we investigate in detail the possibility of probing those aspects through the observables classified in the previous section by considering the cases without and with direct reconstruction of the production plane separately.

### 4.1.1 Without direct reconstruction of the production plane

If the production plane is not directly reconstructed but only the helicities of the produced top quark and anti–quark are statistically determined, all the interference between the scalar and vector contributions is averaged away over the azimuthal angle  $\Phi$  and only the observables,  $\{C_1, C_2, C_3, C_4, C_{15}, C_{16}; D_1, D_2, D_3, D_4\}$  can be reconstructed.

Figures 3 and 4 exhibit six independent cross sections of definite CP and  $CP\tilde{T}$  parities near the region of the heavy Higgs–boson resonances;

$$(a) \sigma_{RL}[++], \quad (b) \sigma_{LR}[++], \quad (c)/(d) \frac{\sigma_{RR} \pm \sigma_{LL}}{2}[\pm\pm], \quad (e) \sigma_{\parallel}[++], \quad (f) \sigma_{\perp}[-+],$$

for  $\tan\beta = 3, 10$  in Figs. 3 and 4, respectively. The cross sections obtained by controlling solely the muon and anti–muon polarizations are given by

$$\begin{aligned} \sigma_{RL/LR} &= \frac{N_C \beta}{16 \pi s} \int d \cos \Theta [C_1 \pm C_2] , \\ \sigma_{RR/LL} &= \frac{N_C \beta}{8 \pi s} [C_3 \pm C_4] , \\ \sigma_{\parallel/\perp} &= \frac{N_C \beta}{16 \pi s} (\pm) C_{15/16} . \end{aligned} \tag{48}$$

---

<sup>‡</sup>The  $b\bar{b}$  decay mode of the lightest Higgs boson, even if it has the largest branching fraction, is not useful for certain observables because of the difficulty in determining the polarization and electric charge of the produced bottom quark and anti–quark experimentally.

As shown in the frames (a) and (b) the spin-1 (LR) and (RL) cross sections  $\sigma_{LR}$  and  $\sigma_{RL}$  in both figures are almost constant and the former is almost twice larger than the latter, showing the large left-right asymmetry. On the other hand, the average of the cross sections  $\sigma_{LL}$  and  $\sigma_{RR}$  showing the Higgs-boson contributions are peaked on each heavy Higgs-boson resonance and the size at each pole is comparable to that of the spin-1 cross section. In the CP invariant case ( $\Phi_{A\mu} = 0$ ) with  $\tan\beta = 3$  the parameter set (46) with  $\tan\beta = 3$  accidentally generates two extremely degenerate Higgs bosons as denoted by a single resonance line in the frame (c) as well as a single oscillating pattern in the frame (e) for  $\sigma_{\parallel}$  of Fig. 3 unlike the case for  $\tan\beta = 10$  with a finite mass splitting of about 3 GeV. The CP-odd observables  $(\sigma_{RR} - \sigma_{LL})/2$  and  $\sigma_{\perp}$  are identically zero for both  $\tan\beta = 3$  and 10 as they ought to be. On the other hand, in the CP non-invariant case a large mass splitting between two Higgs-boson resonances is developed for  $\tan\beta = 3$ , implying a large CP-violating mixing between two Higgs bosons, while the splitting in the case of  $\tan\beta = 10$  is not so much enlarged. A more quantitative understanding about the mass splitting can be obtained from Eq. (47). In this case, the CP-odd observables are non-vanishing. Note that observable  $\sigma_{\perp}$  are quite sizable on the poles, especially, in the case of  $\tan\beta = 3$ .

The observable  $(\sigma_{RR} - \sigma_{LL})/2$  in the frame (d) is CPT-odd, involving the propagator combination  $\mathcal{D}_{kl}$ , but the observables  $\sigma_{\parallel}$  and  $\sigma_{\perp}$  in the frames (e) and (f) are CPT-even, involving the propagator combination  $\mathcal{S}_{kl}$ . Examining the analytic structure of those observables and taking into account the parameter set (46), we find that (i) the coefficient related with the CP-odd (CP-even) resonance pole is negative (positive), respectively; (ii) for  $\tan\beta = 3$  the lighter (heavier) resonance of the heavy Higgs bosons is dominantly CP-odd (CP-even) in both the CP invariant and non-invariant cases, respectively; (iii) for  $\tan\beta = 10$  the lighter resonance is dominantly CP-even (CP-odd) and the heavier one CP-odd (CP-even) in the CP invariant (non-invariant) case for  $\Phi_{A\mu} = 0$  ( $\pi/2$ ), respectively. Combining all these features leads to a symmetric resonance pattern in the frame (d) and anti-symmetric patterns in the frames (e) and (f) in both figures and a remarkable sign flipping at each resonance pole in the frame (e) of Fig. 4.

We present in Fig. 5 three observables<sup>§</sup> related with the difference between the cross sections with the (++) and (--) helicity configurations:

$$\frac{\Delta_{RR} - \Delta_{LL}}{2}[++], \quad \Delta_{\perp}[+-], \quad \Delta_{\parallel}[--],$$

near the heavy Higgs-boson resonances, the explicit form of which is obtained by integrating

---

<sup>§</sup>The sum  $\Delta_{RR} + \Delta_{LL}$  is strongly suppressed in the present case due to the orthogonality of the neutral-Higgs mixing matrix  $O$ :  $\sin\beta$  is very close to unity even for  $\tan\beta = 3$  such that the product sum  $O_{2k}O_{2l} + s_{\beta}^2 O_{1k}O_{1l}$  is approximately  $\delta_{kl}$ , i.e. vanishing in the present case because of  $k \neq l$  forced by the antisymmetric combination  $O_{1k}S_l^f - S_k^f O_{1l}$  with  $S_l^f = O_{3l}$  for  $f = t$ .

the distributions  $\{D_2, D_3, D_4\}$  over the production angles as

$$\Delta_{RR/LL} = \frac{N_C \beta}{8 \pi s} [D_1 \pm D_2], \quad \Delta_{\parallel/\perp} = \frac{N_C \beta}{16 \pi s} D_{3/4}. \quad (49)$$

It should be noted that every observable  $D_i$  ( $i = 1$  to 4) involves the antisymmetric combination  $(O_{1k}O_{3l} - O_{3k}O_{1l})$  forcing  $k \neq l$  ( $k, l = 1, 2, 3$ ). Because two heavy Higgs bosons exhibit almost a typical two-state mixing for the parameter set (46), there exist simply one coupling combination formed by the mixing matrix elements for each observable. As a result, the  $\sqrt{s}$  dependence of each observable is (almost) completely determined by that of the propagator combinations  $\mathcal{S}_{23}$  or  $\mathcal{D}_{23}$ , depending on whether the observable is  $\text{CPT}$ -even or  $\text{CPT}$ -odd. As two Higgs bosons are extremely degenerate in the CP invariant case with  $\tan \beta = 3$  a single resonance peak (solid line) is shown in the first two upper frames of Fig. 5. However, we note in the upper part of Fig. 5 that (i) in the CP non-invariant case ( $\Phi_{A\mu} = \pi/2$ ) a large mass splitting is developed; and (ii) the  $\text{CPT}$ -even observable  $(\Delta_{RR} - \Delta_{LL})/2$  changes its sign at each resonance pole as  $\mathcal{S}_{23}$  does, while the other two  $\text{CPT}$ -odd observables have a two-pole structure of the same sign. On the other hand, the mass splitting between two heavy Higgs bosons for  $\tan \beta = 10$  is not so different in the CP invariant and non-invariant cases. As explained in the case of  $\tan \beta = 3$ , one can see a sign change at each resonance pole in the  $\text{CPT}$ -even observable and a typical two-pole structure in the  $\text{CPT}$ -odd observables. It is also noteworthy that the observable  $\Delta_{\perp}$  is negative (positive) for the CP invariant (non-invariant) case. Finally, the typical size of the CP-odd observables is very small compared to that of the CP-even observables.

#### 4.1.2 With direct reconstruction of the production plane

All the terms involving interference between the scalar and vector contributions requires a reasonable identification of the production plane and they are proportional to the mass of the final fermion. The  $\tau^+\tau^-$  mode with two final neutrinos escaping detection can be used at high energies where the produced tau leptons are very energetic and therefore their decay products fly along the original tau direction to a very good approximation. Nevertheless, the small mass leads to very small interference effects. On the other hand, the production plane in the  $t\bar{t}$  mode can be determined without big difficulty and the top-quark mass is almost 100 times larger than the tau-lepton mass. In this light, we will concentrate on the  $t\bar{t}$  mode which could generate significant interference effects.

Among the eight interference terms the four terms  $\{C_7, C_8, C_9, C_{10}\}$  are CP-odd and the other four terms  $\{C_5, C_6, C_{11}, C_{12}\}$  are CP-even. It is noteworthy that all the CP-odd terms are proportional to  $R_3$  while all the CP-even observables to  $R_1$ ; as a matter of fact the CP properties of the interference terms originates from those of  $R_1$  and  $R_3$  as can be

worked out by their explicit form for the  $t\bar{t}$  mode:

$$R_1 = -2h_\mu h_f \sum_{k=1}^3 D_{H_k} O_{2k} O_{3k}, \quad R_3 = 2ih_\mu h_f s_\beta \sum_{k=1}^3 D_{H_k} O_{1k} O_{3k}. \quad (50)$$

We note that (i)  $R_1$  describes the CP-preserving mixing between two CP-even states,  $\phi_1$  and  $\phi_2$ , so that the relevant observables can be used to select the dominantly CP-even Higgs-boson states; (ii) the coefficients  $O_{22}O_{32}$  and  $O_{23}O_{33}$  have an equal sign while the coefficients  $O_{12}O_{32}$  and  $O_{13}O_{33}$  have an opposite sign; (iii)  $R_3$  the CP-violating mixing between  $\phi_2$  and the CP-odd state  $a$ . In addition, the coefficients  $W_{1,3}$  involving vector bilinear charges are (almost) real to a very good approximation so that the SV interference terms depends on the real and imaginary parts of each Higgs-boson propagator  $D_{H_k}$  itself.

Certainly we need to apply an appropriate  $\Phi$ -dependent weight function to extract each interference term; for example,  $(\cos \alpha - \cos \bar{\alpha})$  with  $P_T = \bar{P}_T = 1$  taken can be used as a weight function to extract  $C_7$ . The extraction efficiency should be determined with the detailed information on various experimental machine parameters. So, we will not provide any further detailed procedure to extract those observables, but concentrate ourselves on the observables  $C_i$  themselves. Let us define the cross sections  $\sigma_i$  ( $i = 5$  to 12) as:

$$\sigma_i = \frac{N_C \beta}{32\pi s} \int d\cos\Theta C_i, \quad (51)$$

so that  $\sigma_i$  has the same CP property as  $C_i$ .

Taking the maximal CP-violating phase  $\Phi_{A\mu} = \pi/2$ , we present in Fig. 6 the CP-odd observables  $\{\sigma_7[- -], \sigma_8[- +], \sigma_9[- -], \sigma_{10}[- +]\}$  for the  $t\bar{t}$  mode near the heavy Higgs-boson resonances for  $\tan\beta = 3$  (solid line) and  $\tan\beta = 10$  (dashed line) with the SUSY parameter set (46). The CPT-even observables  $\sigma_8$  and  $\sigma_{10}$  changes their sign at each pole as the real part of each Higgs-boson propagator changes its sign. On the other hand, the fact that the coefficients  $O_{12}O_{32}$  and  $O_{13}O_{33}$  have an opposite sign is responsible for the sign-flipping pattern at the poles, appearing in the left frames of Fig. 6. On the whole, among those CP-odd observables  $\sigma_7$  and  $\sigma_{10}$  are sizable while the other two observables are small in size.

Figure 7 shows the CP-even observables  $\{\sigma_5[+ +], \sigma_6[+ -], \sigma_{11}[+ +], \sigma_{12}[+ -]\}$  for the  $t\bar{t}$  mode near the heavy Higgs-boson resonances for  $\Phi_{A\mu} = 0$  (solid line) and  $\Phi_{A\mu} = \pi/2$  (dashed line) with the SUSY parameter set (46). In this case, we take  $\tan\beta = 3$  causing a larger CP-violating Higgs-boson mixing than  $\tan\beta = 10$ . As explained before, the observables dependent on the coefficients  $O_{2k}O_{3k}$  single the dominantly CP-even states out. As can be seen in every frame of Fig. 7 the heavier Higgs boson of two heavy Higgs bosons is (dominantly) CP-even in the case of  $\Phi_{A\mu} = 0$  and  $\pi/2$ , respectively. The CPT-even observables  $\sigma_5$  and  $\sigma_{11}$  show a sign change at the Higgs-boson resonance pole, while the CPT-odd observables show a typical peak.

## 4.2 The lightest Higgs boson

According to a detailed analysis [12] of Higgs boson decays, the width of the lightest Higgs boson  $H_1$  is of the order of MeV for intermediate  $\tan\beta$ , which is smaller than a typical muon energy resolution. The lightest Higgs boson decays dominantly into  $b\bar{b}$  and sub-dominantly into  $\tau^+\tau^-$  with the (almost) fixed branching fractions and the interference between the Higgs-exchange and the  $\gamma$  and  $Z$ -boson exchanges is negligible because of the small  $b$  and  $\tau$  masses compared to the Higgs-boson mass, even if the muon beam polarization is employed. Furthermore,  $\Gamma(H_1 \rightarrow f_R \bar{f}_R) = \Gamma(H_1 \rightarrow f_L \bar{f}_L)$  at the tree level so that any further information on the CP property of the lightest Higgs boson will not be obtained by measuring the difference between the final  $(++)$  and  $(--)$  helicity configurations<sup>¶</sup>.

A convolution of the Higgs-boson production cross section with the beam energy distribution tends to reduce the production rate as given by the expression

$$\Sigma_{H_1 eff} \approx \frac{\pi \Gamma_{H_1}}{2\sqrt{2}\pi\sigma_E} \Sigma_{H_1}(m_{H_1}), \quad (52)$$

where  $\sigma_E$  is the muon beam energy resolution and the distribution  $\Sigma_{H_1}$  is given by

$$\Sigma_{H_1}(m_{H_1}) = (1 + P_L \bar{P}_L) C_3 + (P_L + \bar{P}_L) C_4 + P_T \bar{P}_T [\cos \eta C_{15} - \sin \eta C_{16}]. \quad (53)$$

Every  $C_i$  is proportional to the second power of  $m_{H_1}/\Gamma_{H_1}$  and factored into the production and decay parts on the lightest Higgs-boson resonance pole. So, apart from the factor depending on the beam energy resolution, the CP property of the lightest Higgs boson can be directly investigated through the Higgs-boson resonance production by polarized muon and anti-muon collisions as well as through final fermion spin-spin correlations with high efficiencies. The reduction factor in Eq. (52) clearly shows the importance of having a very good beam energy resolution in order to obtain the spin-0 Higgs-exchange signal events clearly distinguished from the spin-1  $\gamma/Z$ -exchange background events. Since several works [13, 16, 17] along this line have been already done, we close this section to referring to the relevant recent works.

## 5 Summary and Conclusion

We have performed a systematic investigation of the production of a third-generation fermion-pair in polarized  $\mu^+\mu^-$  collisions so as to probe the explicit CP violation in the MSSM Higgs sector, induced radiatively by soft trilinear interactions related to squarks of the third generation. We have classified all the observables for probing the CP property of

---

<sup>¶</sup>The identification of the  $\tau^+\tau^-$  helicities is, however, quite useful to reduce the continuum backgrounds from the  $\gamma$  and  $Z$  exchanges [23].

the Higgs bosons constructed by the initial muon beam polarization along with the final fermions of no polarization and of equal helicity, respectively. The polarization observables have turned out to allow for complete determination of the CP property of the Higgs bosons. Furthermore, we have found that the interference between the spin-0 Higgs-boson and spin-1  $\gamma/Z$  contributions can provide a powerful and independent means for the determination of the CP property of two heavy Higgs boson in the top-quark pair production with the c.m. energy near the (almost) degenerate heavy Higgs-boson resonances. On the other hand, there is no sizable interference between the lightest Higgs-boson and spin-1  $\gamma/Z$  contributions so that the CP property of the lightest Higgs boson can be optimally measured on its pole by using the initial muon beam polarization or the final fermion spin-spin correlations with high efficiencies while keeping a very good beam energy resolution.

In conclusion, the third-generation fermion-pair production in  $\mu^+\mu^-$  collisions equipped with initial muon beam polarization and final-fermion spin correlations provides a powerful probe of the CP property of the Higgs bosons in the MSSM with explicit CP violation.

## Acknowledgements

S.Y.C wishes to acknowledge financial support of the 1997 Sughak program of the Korea Research Foundation. E.A thanks KIAS for the great hospitality extended to her while this work was beeing performed.

## References

- [1] See, J.F. Gunion, H.E. Haber, G. Kane and S. Dawson, ‘*Higgs Hunter’s Guide*’, Addison-Wesley Publishing Company, (1990), and references therein; M. Spira and P.M. Zerwas, hep-ph/9803257.
- [2] J.H. Christenson, J.W. Cronin, V.L. Fitch and R. Turlay, Phys. Rev. Lett. **13**, 138 (1964); for reviews, see, for example, P.K. Kabir, *The CP Puzzle*, (Academic Press, London and New York, 1968); W. Grimus, Fortschr. Phys. **36**, 201 (1988); E.A. Paschos and U. Türke, Phys. Rep. **178**, 147 (1989); B. Winstein and L. Wolfenstein, Rev. Mod. Phys. **65**, 1113 (1993); G.D. Barr *et al.*, NA31 Collaboration, Phys. Lett. **B317**, 233 (1993); A. Alavi-Harati *et al.*, KTeV Collaboration, Phys. Rev. Lett. **83**, 22 (1999); V. Fanti *et al.*, NA48 Collaboration, Phys. Lett. **B465**, 335 (1999).
- [3] For pedagogical introduction to CP violation in the B-meson system, see M. Neubert, Int. J. Mod. Phys. **A11**, 4173 (1996); A.J. Buras, hep-ph/9806471 and references therein.

- [4] N. Ruis and V. Sanz, Nucl. Phys. **B570**, 155 (2000) and references therein.
- [5] A. Pilaftsis, Phys. Lett. **B435**, 88 (1998), hep-ph/9805373; Phys. Rev. **D58**, 096010 (1998), hep-ph/9803297.
- [6] A. Pilaftsis and C.E.M. Wagner, Nucl. Phys. **B553**, 3 (1999), hep-ph/9803297.
- [7] D.A. Demir, Phys. Rev. **D60**, 055006 (1999), hep-ph/9901389.
- [8] S.Y. Choi, M. Drees and J.S. Lee, hep-ph/0002287 (to appear in Phys. Lett. B).
- [9] M. Carena, J. Ellis, A. Pilaftsis and C.E.M. Wagner, hep-ph/0003180.
- [10] D. Chang, W.-Y. Keung and A. Pilaftsis, Phys. Rev. Lett. **82**, 900 (1999), erratum: **83**, 3972 (1999), hep-ph/9811202; A. Pilaftsis, Phys. Lett. **B471**, 174 (1999), hep-ph/9909485.
- [11] A. Pilaftsis, Phys. Rev. Lett. **77**, 4996 (1997), hep-ph/9603328; K.S. Babu, C. Kolda, J. March-Russell and F. Wilczek, Phys. Rev. **D59**, 016004 (1999), hep-ph/9804355; S.Y. Choi and M. Drees, Phys. Rev. Lett. **81**, 5509 (1998), hep-ph/9808377; J.F. Gunion and J. Pliszka, Phys. Lett. **B444**, 136 (1998), hep-ph/9809306; C.A. Boe, O.M. Ogreid, P. Osland and J. Zhang, Eur. Phys. J. **C9**, 413 (1999), hep-ph/9811505; B. Grzadkowski, J.F. Gunion and J. Kalinowski, Phys. Rev. **D60**, 075011 (1999), hep-ph/9902308.
- [12] S.Y. Choi and J.S. Lee, Phys. Rev. **D61**, 015003 (2000), hep-ph/9907496.
- [13] S.Y. Choi and J.S. Lee, hep-ph/9909315 (to appear in Phys. Rev. D); hep-ph/9910557 (to appear in Phys. Rev. D); hep-ph/9912330 (to appear in Phys. Rev. D).
- [14] V. Barger, M.S. Berger, J.F. Gunion and T. Han, Phys. Rep. **281**, 1 (1997).
- [15] V. Barger, M.S. Berger, J.F. Gunion, and T. Han, Phys. Rev. Lett. **75**, 1462 (1995); J.F. Gunion, in *Proceedings of the 5th International Conference on Physics Beyond the Standard Model, Balholm, Norway, 1997*, edited by G. Eigen, P. Osland and B. Stugu (AIP, Woodbury, New York, 1997), p. 234.
- [16] D. Atwood and A. Soni, Phys. Rev. D **52**, 6271 (1995); A. Pilaftsis, Phys. Rev. Lett. **77**, 4996 (1996); Nucl. Phys. **B504**, 61 (1997); S.Y. Choi and M. Drees, Phys. Rev. Lett. **81**, 5509 (1998).
- [17] B. Grzadkowski, J.F. Gunion and J. Pliszka, hep-ph/0003091; hep-ph/0004034 and references therein.



- [18] E. Asakawa, A. Sugamoto, J. Kamoshita and I. Watanabe, hep-ph/9912373 (to appear in Eur. Phys. J. C); E. Asakawa, A. Sugamoto and I. Watanabe, hep-ph/0004005.
- [19] S. Dimopoulos and D. Sutter, Nucl. Phys. **B 452** (1995) 496; H. Haber, Proceedings of the 5th International Conference on Supersymmetries in Physics (SUSY'97), May 1997, ed. M. Cvetič and P. Langacker, hep-ph/9709450.
- [20] S. Coleman and E. Weinberg, Phys. Rev. **D7**, 1888 (1973); Y. Okada, M. Yamaguchi and T. Yanagida, Prog. Theor. Phys. **85**, 1 (1991); Phys. Lett. **B262**, 54 (1991); J. Ellis, G. Ridolfi and F. Zwirner, Phys. Lett. **B257**, 83 (1991); **B262**, 477 (1991).
- [21] K. Hagiwara and D. Zeppenfeld, Nucl. Phys. **B274**, 1 (1986).
- [22] L.M. Sehgal and P.M. Zerwas, Nucl. Phys. **B183**, 417 (1981).
- [23] V. Barger, T. Han and C.-G. Zhou, hep-ph/0002042 (to appear in Phys. Lett. B).

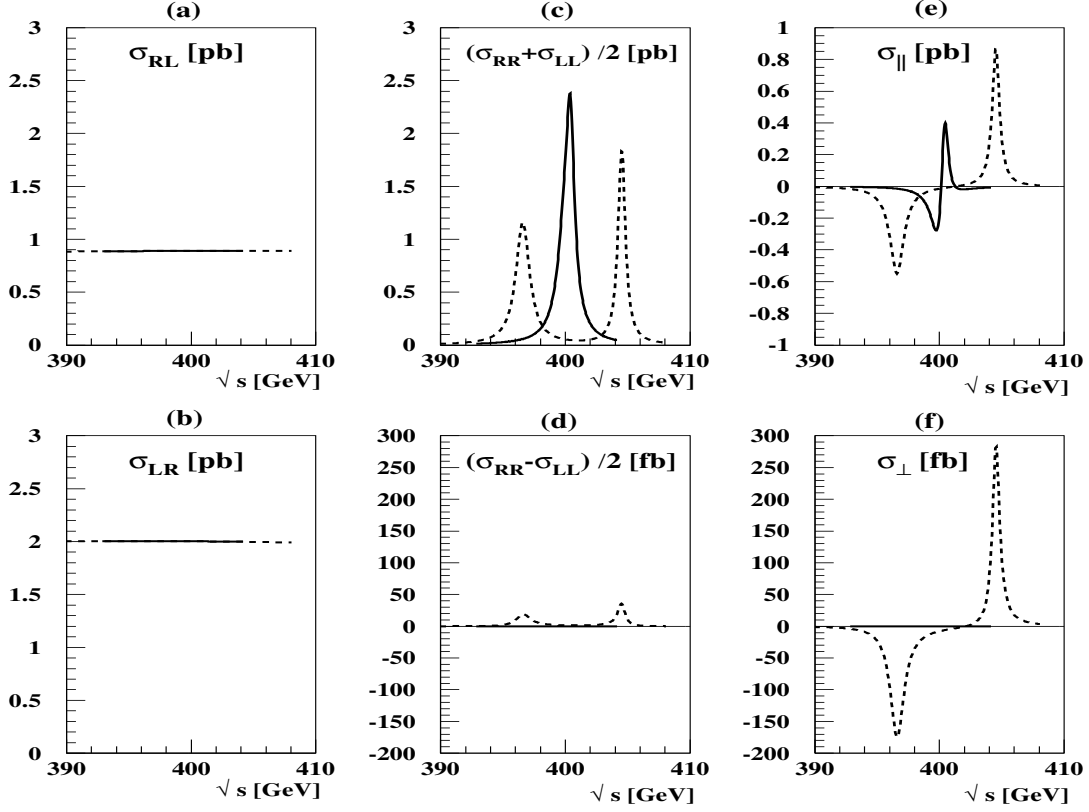


**Figure 3:** The six independent cross sections of definite  $CP$  and  $CPT$  parities; (a)  $\sigma_{RL}[++]$ , (b)  $\sigma_{LR}[++]$ , (c)  $[\sigma_{RR} + \sigma_{LL}]/2[++]$ , (d)  $[\sigma_{RR} - \sigma_{LL}]/2[--]$ , (e)  $\sigma_{||}[++]$  and (f)  $\sigma_{\perp}[-+]$ , near the region of the heavy Higgs-boson resonances for  $\tan\beta = 3$  and the SUSY parameter set (46). The definition of the cross sections is given in Eq. (48). The solid line is for  $\Phi_{A\mu} = 0$  and the dashed line for  $\Phi_{A\mu} = \pi/2$ .

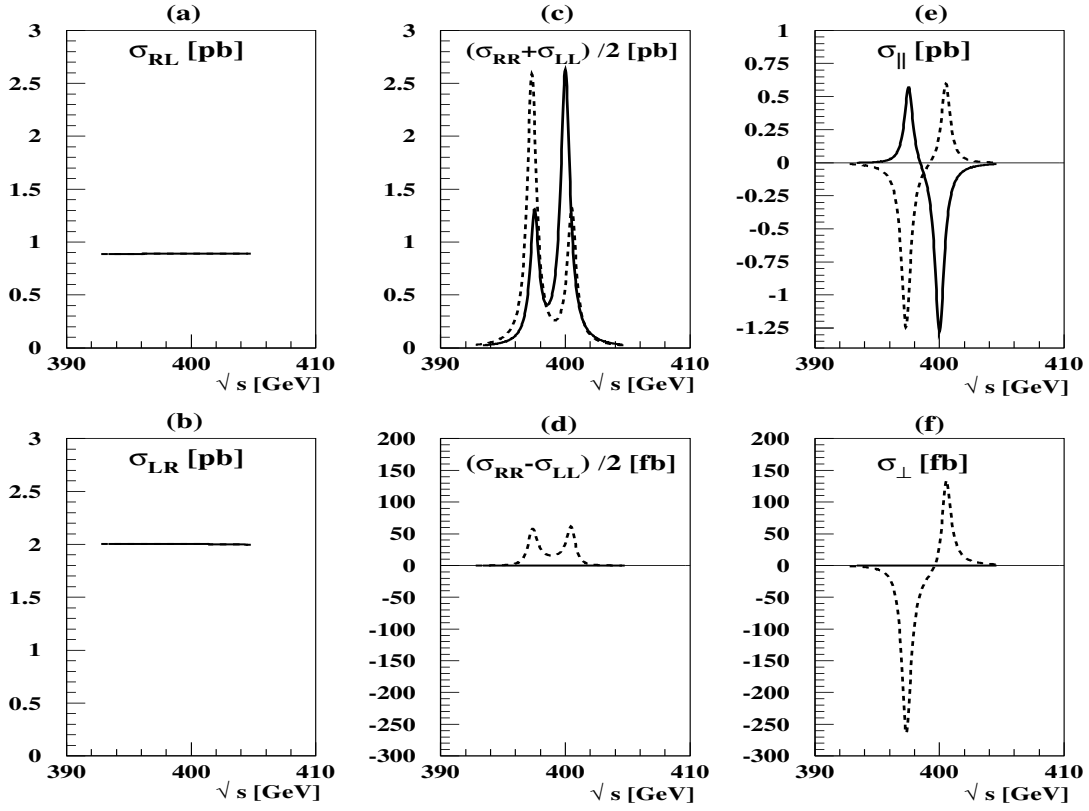


**Figure 4:** The same six independent cross sections as in Fig. 3 near the region of the heavy Higgs-boson resonances for  $\tan\beta = 10$  and the SUSY parameter set (46). The solid line is for  $\Phi_{A\mu} = 0$  and the dashed line for  $\Phi_{A\mu} = \pi/2$ .

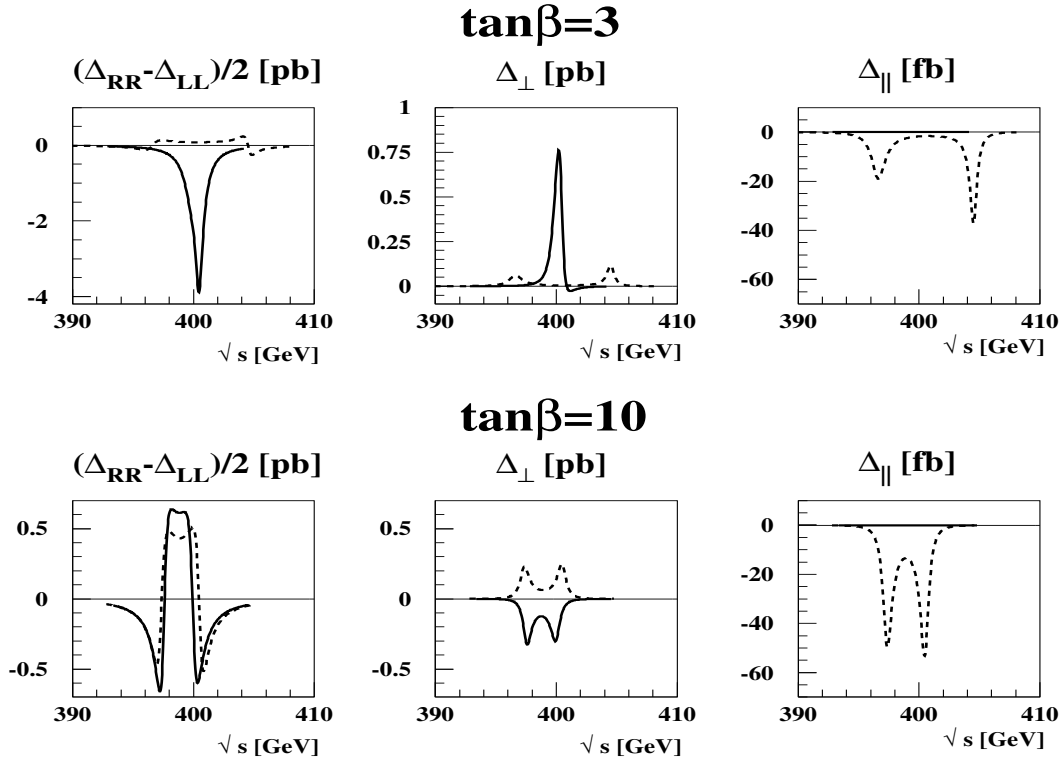


**Figure 5:** The three cross sections of definite  $CP$  and  $CPT$  parities;  $[\Delta_{RR} - \Delta_{LL}]/2[++]$  (left),  $\Delta_{\perp}[+-]$  (middle), and  $\Delta_{\parallel}[- -]$  (right) near the region of the heavy Higgs-boson resonances for  $\tan\beta = 3$  (upper set) and  $\tan\beta = 10$  (lower set) with the SUSY parameter set (46). The definition of the cross sections is given in Eq. (49). The solid line is for  $\Phi_{A\mu} = 0$  and the dashed line for  $\Phi_{A\mu} = \pi/2$ .

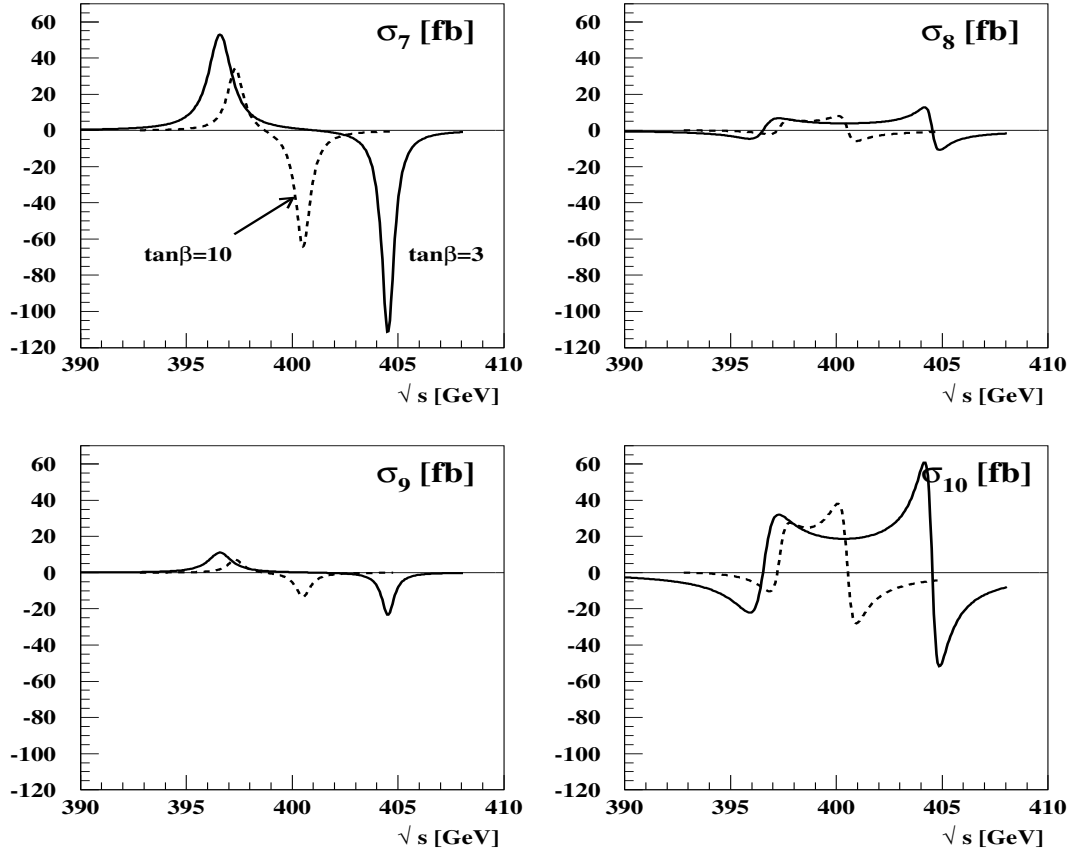


**Figure 6:** The four CP-odd cross sections  $\{\sigma_7[--], \sigma_8[-+], \sigma_9[--], \sigma_{10}[-+]\}$  for the  $t\bar{t}$  mode near the heavy Higgs-boson resonances with the SUSY parameter set (46). The solid line is for  $\tan\beta = 3$  and the dashed line for  $\tan\beta = 10$ . The definition of the cross sections is given in Eq. (51). The CP phase  $\Phi_{A\mu}$  is taken to  $\pi/2$ .

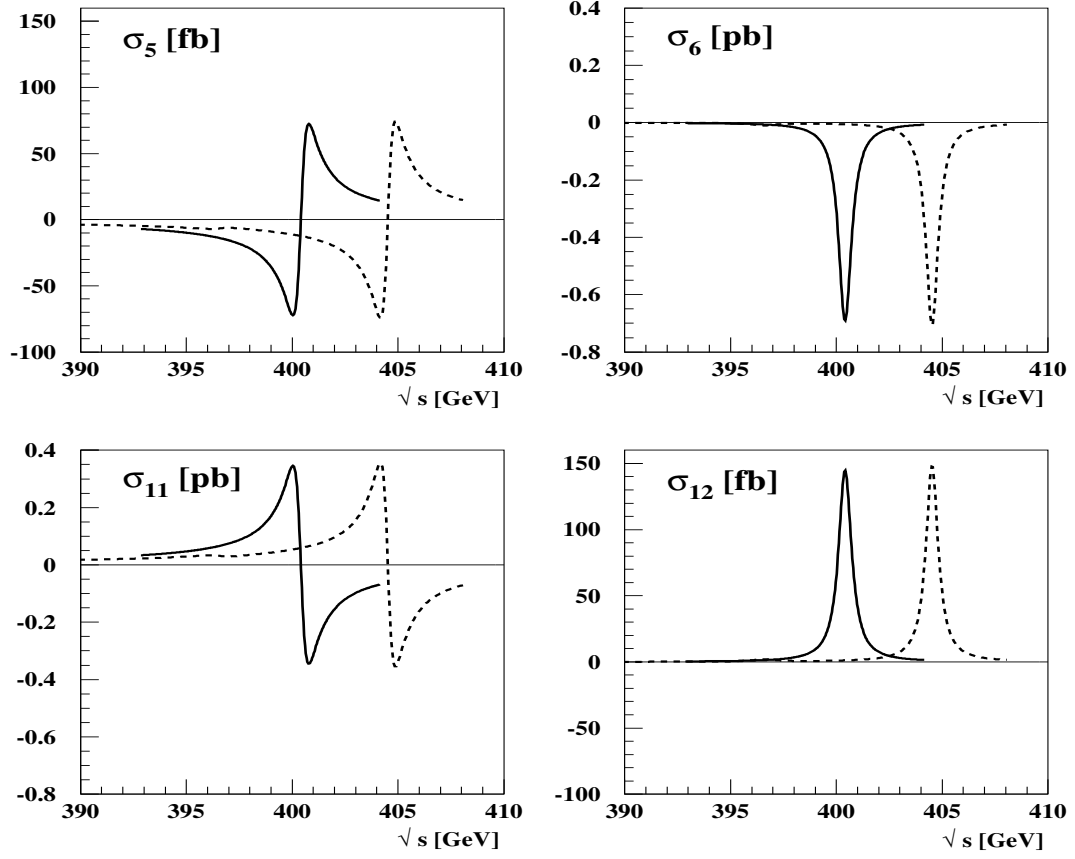


**Figure 7:** The four  $CP$ -even cross sections  $\{\sigma_5[++], \sigma_6[+-], \sigma_{11}[++], \sigma_{12}[+-]\}$  for the  $t\bar{t}$  mode near the heavy Higgs-boson resonances for  $\tan\beta = 3$  with the SUSY parameter set (46). The solid line is for  $\Phi_{A\mu} = 0$  and the dashed line for  $\Phi_{A\mu} = \pi/2$ . The definition of the cross sections is given in Eq. (51).